THE JOURNAL OF PHYSICAL CHEMISTRY Letters

Letter

pubs.acs.org/JPCL

Conditions for Directional Charge Transfer in CdSe Quantum Dots Functionalized by Ru(II) Polypyridine Complexes

Svetlana Kilina,*[,†] Peng Cui,[‡] Sean A. Fischer,[§] and Sergei Tretiak[∥]

[†]Department of Chemistry and Biochemistry, North Dakota State University, Fargo, North Dakota 58108, United States

[‡]Materials and Nanotechnology Program, North Dakota State University, Fargo, North Dakota 58108, United States

[§]Department of Chemistry, University of Washington, Seattle, Washington 98195, United States

[∥]Theoretical Division (T-1) and Center for Integrated Nanotechnologies, Los Alamos National Laboratory, Los Alamos, New Mexico 87545, United States

Supporting Information

ABSTRACT: Thermodynamic conditions governing the charge transfer direction in CdSe quantum dots (QD) functionalized by either Ru(II)-trisbipyridine or black dye are studied using density functional theory (DFT) and time-dependent DFT (TDDFT). Compared to the energy offsets of the isolated QD and the dye, QD−dye interactions strongly stabilize dye orbitals with respect to the QD states, while the surface chemistry of the QD has a minor effect on the energy offsets. In all considered QD/dye composites, the dyes always introduce unoccupied states close to the edge of the conduction band and control the electron transfer. Negatively charged ligands and less polar solvents significantly destabilize the dye's occupied orbitals shifting them toward the very edge of the valence band, thus, providing favorite conditions for the hole transfer. Overall, variations in the dye's ligands and solvent polarity can progressively adjust the electronic structure of QD/dye composites to modify conditions for the directed charge transfer.

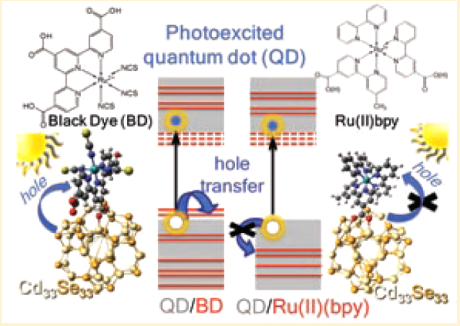

SECTION: Molecular Structure, Quantum Chemistry, and General Theory

Efficient harvesting and conversion of solar energy to electrical or chemical energy relies on the charge separation process that prevents carrier recombination prior to their extraction to contacts. Application of molecular adsorbents forms the interface between two different media, one acting as an electron donor, and another as an acceptor. As such, this interface facilitates a quick separation of the photogenerated carriers before carrier annihilation or energy dissipation takes place, while not requiring high-quality materials as in conventional Si-based solar cells.[1,2] This concept was first realized in the dye-sensitized solar cells, so-called Grätzel cells.[3−5]In these devices, a molecular dye—typically a chemical derivative of ruthenium(II) polybipyridine (Ru(II)-bpy)—is used as a sensitizer that absorbs visible light and then injects electrons into the large-bandgap semiconductor TiO_2. Another working scenario suggests a substitution of the TiO_2 semiconductor by nanocomposites, e.g., arrays of semiconductor quantum dots (QDs), acting as acceptors of electrons from photoexcited dyes.[1,6] In this case, the prospect of having the ability to fabricate ultrathin, light, and flexible nanomaterials, as well as taking advantage of the size-tunable electronic properties of QDs, could be beneficial for the optimization of the work functions of devices,[7] making the QD-based dye-sensitized solar cells more attractive than Grätzel cells based on bulk semiconductors.

Ruthenium(II) polypyridine complexes and tris(2,2′-bipyridine) Ru(II) ($[Ru(bpy)_3]^{2+}$), in particular, are commonly used in these photovoltaic applications because of their unique combination of chemical stability, strong visible absorption, excited-state reactivity, and redox properties responsible for charge transfer.[8] These properties also allow for the use of the semiconductor−Ru(II)-complex assemblies as a photo-oxidizing agent. In particular, Meyer and co-workers[9] have demonstrated that in appropriately modified Ru(II) complexes, the oxidizing equivalents stored in the complex following the electron injection into TiO_2 can be used to drive chemical processes such as catalytic oxidation of organic substrates. An alternative approach for possible usage of Ru(II) complexes as photo-oxidizers has been proposed based on assemblies of Ru(II)bpy complexes and CdSe QDs.[10] In these nanoassemblies, the QD rather than the complex is suggested to function as a light-harvesting and charge generating component, offering better photostability and size-tunable absorption.

A similar idea of using QDs as a sensitizer substituting for molecular dyes has been recently realized for semiconductor-sensitized solar cells.[7] Just as in the QD-based photocatalytic agents, utilization of QDs in solar cells promises higher

Received: September 25, 2014
Accepted: September 30, 2014
Published: September 30, 2014

   dx.doi.org/10.1021/jz502017u | J. Phys. Chem. Lett. 2014, 5, 3565−3576

photostability and more efficient light absorption that can be tuned over a broad wavelength range. Additionally, the ability to generate multiple excited electron−hole pairs from a single photon, so-called carrier multiplication,[11] promises significantly improved performance of photovoltaic devices.[12,13] However, despite these potential advantages, power conversion efficiencies of QD-sensitized solar cells so far do not exceed 5%. Such relatively low performance is attributed to very rapid carrier recombination processes in these materials.[14] To slow down electron−hole recombination, one can introduce structural modifications that will facilitate the hole transfer from the QD-sensitizer. For example, Ru(II)-polypyridyl (N719) and Ru(II)-terpyridine (the black dye) have been shown to act as electron donors[15,16] by activating the hole transfer from the photoexcited QD to the dye. This prevents the electron−hole recombination between the transferred electron at the TiO_2 surface and the trapped hole in the QD.[15,16] Overall, QD-dye assemblies have a great promise to serve as an important element for both solar-to-electrical and solar-to-chemical energy conversion. In both types of applications, conditions and mechanisms of the charge transfer from the photoexcited QD to the dye or backward play a crucial role in the device performance.

While demonstrations of efficient devices have not yet been reported, considerable amounts of effort are now centered on proof-of-concept studies with the main focus on understanding the mechanisms of charge transfer and its competing processes. The latter include electron−hole recombination and energy transfer (i.e., when the electron−hole pair is transferred simultaneously). Different organic and metal−organic dyes have been experimentally studied as functional groups for CdSe,[10,16−19] PbS,[20,21] and ZnO[6] QDs to facilitate various charge transfer processes in these composites. It was shown that the transfer of the photoexcited hole from the QD to the dye, as well as the photoexcited electron from the dye to the QD, depends on the QD size,[10] chemical composition,[6] the complex type[19] and its interaction with the QD surface.[17,22]

Because the mechanisms and kinetics of charge and energy transfer and electron−hole recombination in these nanocomposites are extremely sensitive to the complicated surface chemistry of QDs, a fundamental understanding of these competitive processes is still incomplete. Experimentally, this task is difficult to address: typically electronic states associated with surface defects, impurities and QD-dye interactions are optically forbidden and cannot be probed by conventional spectroscopic means. Moreover, strongly overlapping absorption peaks of different molecular components greatly complicate identification of photoinduced carrier transport properties. It was experimentally observed that over 10 dye molecules can be adsorbed on a single QD.[23] This makes the system even more complex in terms of QD−dye interactions, as well as assembly light interactions. Overall, it is well understood that a delicate interplay between processes taking place at the QD surface controls the efficiency of light conversion to electrical or chemical energy in QD-based devices. As such, understanding the surface chemistry of QDs, in general, and to what extent we can control the photophysics of QDs by chemical functionalization, in particular, is an important prerequisite for optimization of materials for energy conversion applications.

Here, we theoretically elucidate the effect of different ligands in the Ru(II)-complexes on the relative alignments of the energy levels associated with the QD and the dye by performing first-principle, atomistic calculations such as density functional theory (DFT) and time dependent DFT (TDDFT). The energetic alignment between the donor and acceptor states provides insights in thermodynamic conditions and, thus, possible direction of the charge transfer in these complexes. As such, our DFT simulations of the geometries, electronic structures, and optical responses of model CdSe QDs functionalized by Ru(II) trisbipyridine and the black dye, illustrated in Figure 1, allows us to elucidate the charge transfer trends in these systems as a function of Ru-complex ligand.

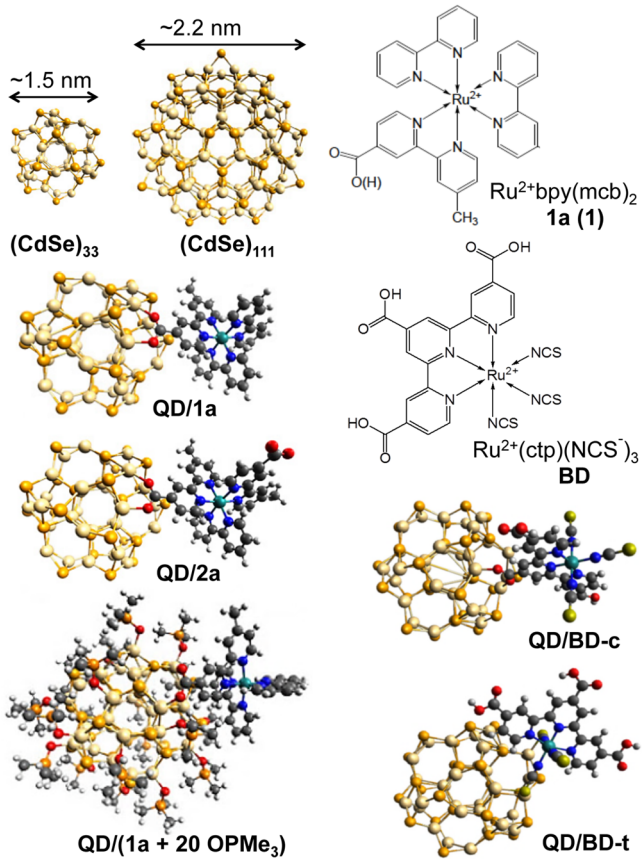

Figure 1. Structures of the systems we studied. Top left panel shows the optimized geometries of the magic size $Cd_{33}Se_{33}$ and $Cd_{111}Se_{111}$ QDs. Left bottom panels present optimized geometries of the $Cd_{33}Se_{33}$ functionalized by the Ru(II)−polybipyridine complexes with one (**QD/1a**) and two (**QD/2a**) carboxylate groups in the absence and in the presence (**QD/(1a+20 OPMe$_3$)**) of passivating ligands, trimethyl-phosphine oxide ($OPMe_3$). On the right, top two panels schematically represent the chemical structure of the Ru(II)−polybipiridine (protonated **2** and deprotonated **2a**) and the black dye (**BD**). Bottom right panels show the $Cd_{33}Se_{33}$ functionalized by the black dye attached via the carboxylate (**QD/BD-c**) and isothiocyanate (**QD/BD-t**) groups.

Computational modeling based on DFT and TDDFT has already been shown as a reliable tool in studies of interactions between QDs and various molecules adsorbed on the QD surface,[24−28] providing important insights on the role of surface ligands in radiative[29−31] and nonradiative[32,33] photoexcited processes of CdSe QDs. Our previous joint experimental and DFT studies[34] have determined the mechanism of attachment of Ru(II)bpy to the CdSe QD surface, elucidating the exclusive attachment of the complex to the Cd sites of the QD surface via a bridging geometry, with the carboxylic anchoring group on

dx.doi.org/10.1021/jz502017u | J. Phys. Chem. Lett. 2014, 5, 3565−3576

the bipyridines being deprotonated in the process. Our very recent calculations[26] have revealed, however, that independent of the complex attachment and the type and size of the QD (PbSe or ZnO of 1 or 2 nm in size), the Ru(II)bpy complex introduces unoccupied orbitals near the band gap of the QD, while the occupied orbitals localized on the Ru(II) ion are located deep inside the QD's valence band. Such energy alignment of the complex and QD orbitals makes the hole transfer from the photoexcited QD to the complex energetically unfavorable.

In this Letter, we show that QD−dye interactions strongly stabilize dye electronic orbitals with respect to the QD states, compared to the energy offsets of the isolated QD and the dye. A negative charge on the ligands coordinated with the metal ion, like a thiocyanate ligand in the black dye, results in a shift of the orbitals originated from the complex toward the very edge of the valence band of the CdSe QD, and makes the hole transfer more favorable. In addition, our calculations predict that a polar solvent can be used to tune the mutual alignment of the dye's and QD's orbitals in order to improve efficiency of the charge transfer. Thus, these results potentially facilitate rational design of organometallic dyes to better control the dye−QD interactions and, consequently, the photophysics of QDs via chemical functionalization.

Description of Systems. We start with the construction of roughly spherical, "magic" size $Cd_{33}Se_{33}$ and $Cd_{111}Se_{111}$ clusters (Figure 1) with the wurtzite crystal symmetry and diameters of about 1.5 and 2.2 nm, respectively, in accordance to the procedure reported in the literature.[27−29,35] The $Cd_{33}Se_{33}$ "magic" structure has been experimentally shown to be stable,[36] while it is the smallest cluster that supports a crystalline-like core of the QD.[37] Our larger $Cd_{111}Se_{111}$ model is even closer to the typical size of QDs in experimental samples. In fact, colloidal CdSe QDs with the average grain diameter of 1.84−2.27 nm, which have an efficient light emission at the wavelength of 500−560 nm, were recently synthesized and investigated.[38]

Experimental studies have demonstrated that the surface passivating layer of CdSe QDs can be effectively functionalized with Ru(II) polypyridine complexes, such as Ru(II)bpy[10,34] and the black dye.[15,16] In these molecules, addition of one or several carboxyl groups at the ligand sites provides at the ligand sites provide chemical bonding of the complex to the QD surface. Therefore, here we focus on two different types of Ru(II) complexes. One molecule includes only 2,2′-bipyridine ligands (bpy) functionalized by one (complex **1**) and two (complex **2**) carboxylic acid and methyl groups (mcb) in their completely deprotonated (**1a** and **2a**) or protonated (**1** and **2**) forms, similar to those experimentally studied in refs 10 and 34. We also model similar Ru(II)bpy complexes with three (complex **3a**) and four (complex **4a**) deprotonated carboxylic acid groups, as illustrated in Figure S1 in the Supporting Information. The second type is the black dye (**BD**) studied in refs 15 and 16, where the Ru(II) ion is coordinated by three isothiocyanate ligands (SCN^-) and the 2,2′:6′,2″-terpyridine (tpy) is functionalized by three carboxyl groups, as illustrated in Figure 1. In addition, we simulate modified versions of the **BD** in which the isothiocyanates are substituted by Cl^- or CO ligands to consider the effect of negatively charged versus neutral ligands on the electronic properties of the QD−dye composites.

The carboxylate linker anchors complexes **1** and **2** to one of the Cd atoms on the QD surfaces via the monodentate attachment (Figure S2 in the Supporting Information). For the deprotonated complexes, the initial attachment is chosen to be the bridging mode, when each oxygen of the carboxylate group is bound to the metal sites of the QD surface (**QD/1a** and **QD/2a** in Figure 1). This attachment has been found to be the most energetically favorable for CdSe-Ru(II)bpy composites.[26,34] For the **BD**, we consider two possible attachments: similar attachment to complexes **1a** and **2a** via the deprotonated carboxylate group in its bridging mode (**BD-c**, Figure 1) and the anchoring via the thiocyanate group (**QD/BD-t**, Figure 1). Protonated complexes **1** and **2** hold a +2 charge due to the Ru(II) ion. Because of negatively charged carboxylate groups, the complex **1a** has a +1 charge, while the complex **2a** is neutral. In contrast, the black dye is negatively charged having −1 and −2 charges in its **BD-t** and **BD-c** forms, respectively, due to the SCN^- groups and deprotonated carboxylate linker.

All complexes are attached to the most chemically reactive surface {1111} (here called the A surface) of the $Cd_{33}Se_{33}$ QD, where all surface cadmiums are 2-coordinated, as discussed in our previous reports.[27,29,34] Nonetheless, bridging attachments of the complex **1a** at the different surfaces of the $Cd_{33}Se_{33}$ cluster (A, B, and D, as illustrated in Figure S2 in the Supporting Information) have been also considered. While multiple Ru(II) polypyridine complexes can be adsorbed on a single QD,[23] here we have to reduce our model to one adsorbed dye molecule on the QD surface to manage the computational cost. Thus, interdye interactions that are possibly present in the real systems are not taken into account in our models. However, our calculations allow us to include the effect of small capping ligands typically present at the QD surface. For this, we have fully passivated the surface of the $Cd_{33}Se_{33}$ cluster by trimethylphosphine oxide ($OPMe_3$) molecules, which are known as a reasonable reduced model[39] for trioctylphosphine oxide (TOPO) ligands commonly used with colloidal CdSe QDs. While the question of the Ru(II) complex binding to the QD surface has been already investigated in detail,[23,26,34] here we focus on the role that a specific ligand coordinated with a Ru(II) ion in the dye plays on the electronic structure and optical properties of the QD/dye composites.

All QD-complex composites together with isolated pristine QDs and Ru(II) complexes are optimized to their lowest-energy configurations at the DFT level of theory in vacuum using the long-range corrected functional CAM-B3LYP, as implemented in the Gaussian-09[40] software package. We utilize the LANL2DZ/6-31G* mixed basis set, where the LANL2DZ basis set is applied to heavy Ru, Cd, and Se atoms and the 6-31G* all-electron basis set is assigned to the rest of the atoms of the ligands. According to our previous investigations, this combination of functional and basis set provides a reasonable description of the structures and QD−ligand binding energies.[27,41] Overall, the increase in the basis set and inclusion of polarization functions have a minor effect on the electronic structure of composites. We have compared the performance of the LANL2DZ/6-31G* basis set (used in the paper for all compounds) with the more extended Def2TZVP basis set, and found an insignificant effect of the increased basis set on both ground state and excited state properties of the complex **1a**, as well as on those of the QD/1a composite. In our previous reports,[27] we have also investigated the effect of the basis set with and without polarization functions on the CdSe QDs passivated by ligands. No significant effect was observed on the

dx.doi.org/10.1021/jz502017u | J. Phys. Chem. Lett. 2014, 5, 3565−3576

electronic and optical properties of the systems, except for the absolute values of the ligand-QD binding energies.

Incorporation of long-rage corrections to the hybrid functional is important for a more appropriate treatment of electronic states with possible charge transfer character, which are typical in metal−organic complexes.[42,43] For example, utilization of the CAM-B3LYP functional results in a decreased number of lower-energy dark states in PbSe and ZnO QDs functionalized by Ru(II)bpy, due to eliminating the well-known problem of "artificial" charge transfer states.[26] On the other hand, long-range corrected functionals are known for their overcorrecting nature of the exciton interactions resulting in optical transition energies of QDs systematically blue-shifted compared to the reference.[44] It is known that the portion of the Hartree−Fock (HF) exchange used in the functional changes the gap: the larger the HF portion, the larger the gap. In other words, tuning the HF portion in the functional, one can adjust the calculated gaps to the experimental ones. Despite a blue shift in the energy due to high portion of the HF exchange, CAM-B3LYP functional has been shown[26] to provide qualitatively similar results to hybrid functionals such as PBE0 and B3LYP, which are able to accurately describe optical gaps of individual CdSe QDs[28,31,44] and Ru(II)bpy complexes.[42,43] For comparison, we have calculated the electronic structure and optical spectra with the B3LYP functional, as well.

Using geometries optimized in vacuum, the electronic structures of all systems studied were calculated in chloroform, benzonitrile, and acetonitrile to elucidate the effect of the solvent polarity. Solvent effects were simulated by embedding the molecule in a polarizable continuum medium (CPCM) with an appropriate dielectric constant using the CPCM reaction field model.[45] The absorption spectra of all systems were calculated using the linear response TDDFT method with the same functional and basis set as used for geometry optimization. Up to 200 singlet states were calculated to model spectra shapes within the energy range of ∼1.5 eV. Gaussian spectral line broadening with an empirical 15 meV width was used to match typical absorption line-shapes observed in experiments.[10,42]

Mutual Energy Alignment of Dye and QD States. Figure 2 shows the projected density of states (PDOS) and, thus, identifies single-electron Kohn−Sham orbitals, which contribute to a specific energy range, as either QD or complex associated states. The unoccupied states belonging to the dyes appear near the edge of the conduction band (CB) independent of the complex, its attachment, its protonated state, or the presence of $OPMe_3$ ligands. These states are mainly localized on the bpy or tpy ligands of the Ru(II) complexes. The 3-D view of these orbitals, shown in Figure 3, confirms their strongly dye-localized nature with negligible traces of orbitals leaking to the QD surface, which explains their weak response to changes in the surface or the anchoring groups. The $OPMe_3$ ligands are found to introduce their electronic states deep inside the conduction and valence (VB) bands of the QD, as marked by the gray line in Figure 2(d). This implies that passivating ligands cause barely any perturbation of the frontier orbitals at the CB edge, as well as at the VB edge.

The occupied orbitals associated with the complex are, however, strongly affected by the type of ligands in the complex. In fact, in complexes **1** and **2**, the dye's occupied orbitals, mostly localized on the Ru(II) ion with a small hybridization over bpy ligands, appear deep inside the VB,

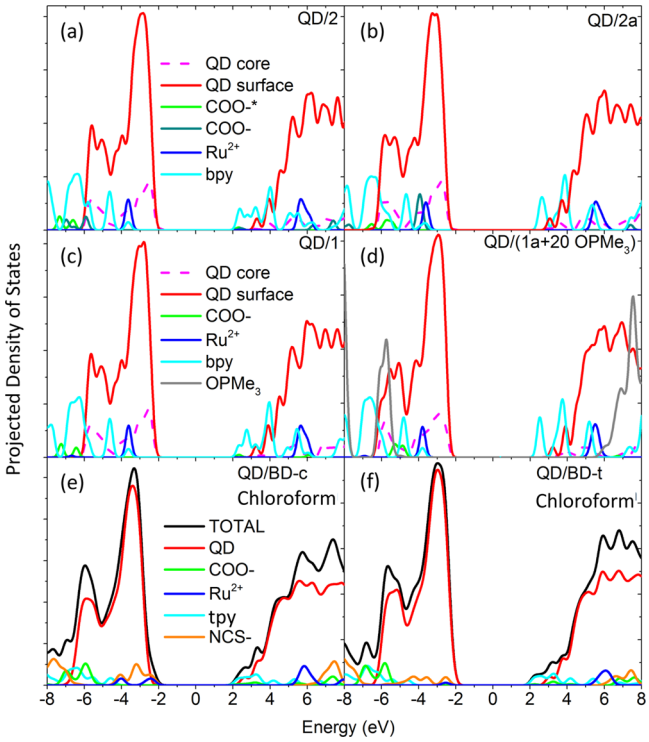

Figure 2. PDOS of the $Cd_{33}Se_{33}$ QD functionalized by derivatives of Ru(II)-bipyridines (a−d) and the black dye (e−f). Calculations are done by CAM-B3LYP functional in chloroform. Zero energy is chosen at the middle of the HOMO−LUMO gap for all systems. The PDOS represents the contributions from the QD's surface (red) and core (dashed magenta) atoms, the Ru(II) ion (blue), the bipyridine (bpy) and terpyridine (tpy) ligands (cyan), the carboxylate (COO) groups (green for nonanchoring and teal for anchoring), thiocyanate groups (orange), and the passivating ligands $OPMe_3$ (gray). The orbitals near the edge of the CB originate from the complex orbitals, independent of the complex. Orbitals associated with Ru(II) ion are deep inside in the VB of the QD functionalized by the Ru(II)-bipyridines, but are at the edge of the QD's VB for the black dye functionalization.

while the edge of the VB is dominated by the QD's states. The protonation of the anchoring carboxyl group and a full coverage of the QD surface by $OPMe_3$ ligands insignificantly changes the relative position of the dye's orbitals versus the QD's states: they stay deep inside the VB of the QD. Such insensitivity originates from a predominantly localized character of Ru(II) orbitals, which have negligible contributions from the carboxylate or the QD atoms, as illustrated in Figure 3, right panel. It is important to note that similar trends in energy alignment of the orbitals of Ru(II)bpy complexes versus the QD's orbitals have been computationally predicted for PbSe and ZnO QDs,[26] demonstrating that the alignment of electronic states is only slightly affected by the chemical composition of the QDs, which does not change the qualitative trends.

When the bipyridine ligands are substituted by the isothiocyanate ligands, the occupied orbitals of **BD** originating from the Ru(II) possess a significant hybridization between the SCN ligands and anchoring carboxyl group, as seen in Figure 3, left panel. As a result, the **BD** orbitals are shifted to the very edge of the VB of the QD, Figure 2e,f. Attachment of the **BD** to the QD surface via the sulfur in the thiocyanate ligand slightly shifts the Ru(II) orbital by ∼0.2 eV toward the VB, pointing to a sensitivity of these states to the dye-QD interactions. Note

dx.doi.org/10.1021/jz502017u | J. Phys. Chem. Lett. 2014, 5, 3565−3576

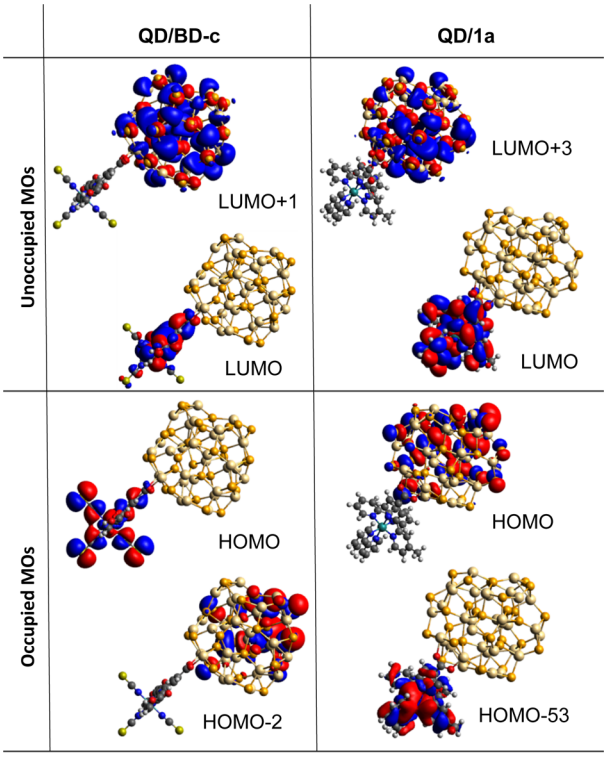

Figure 3. Representative molecular orbitals (MOs) of $Cd_{33}Se_{33}$ QD functionalized by the complex **1a** (right panels) and the black dye (left panels). Calculations are done by CAM-B3LYP functional in chloroform.

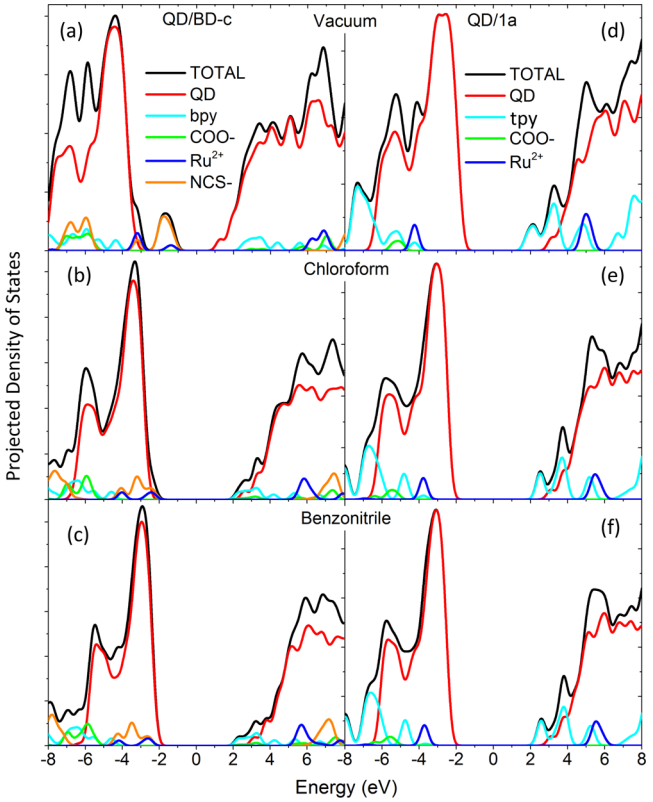

Figure 4. Dependence of the PDOS of $Cd_{33}Se_{33}$ functionalized by the complex **1a** (left panels a–c) and the black dye (right panels d–f) on the solvent polariry. PDOS is calculated by CAM-B3LYP functional in vacuum (a and d), chloroform (b and e) and benzonitrile (c and f). The line colors corresponding to contributions of different parts of systems are kept the same as in Figure 2. Zero energy is chosen at the middle of the HOMO–LUMO gap for all systems.

that the calculated QD-dye binding energy is stronger for **BD-c** with a carboxyl linker (−0.18 eV) than for **BD-t** attached to the QD via the SCN ligand (−0.12 eV), predicting a dominant adsorption of the dye via the carboxyl group. However, even if the less favorable attachment of the **BD-t** happens via the thiocyanate group, the occupied orbitals of the black dye are closer to the VB edge than the orbitals of Ru(II)bpy complexes. As such, the thiocyanate ligands are responsible for aligning the dye's occupied orbitals at the edge of the VB of the QD. Negatively charged thiocyanate ligands destabilize the highest occupied molecular orbital (HOMO) of the complex, lifting it closer or even above the VB edge of the QD.

To better understand the effect of the dye's ligand on the mutual alignment of the molecule's versus the QD's electronic levels, first we investigate the role of the charge on the peripheral groups, carboxylates, which are not directly involved in the coordination with Ru(II) ion. For this, one (**1a**), two (**2a**), three (**3a**), and four (**4a**) deprotonated carboxylic acid groups are added to bipyridine ligands in the Ry(II)bpy complex, resulting in a total charge of +1, 0, −1, and −2, respectively. The chemical structures of all four modified Ru(II)bpy complexes are shown in Figure S1 in the Supporting Information. Independent of the number of the carboxylate groups and the total charge of the complex, the lowest-energy occupied orbitals of the Ru(II)–polypyridine stay inside the VB of the QD, while the dye's unoccupied orbitals contribute to the QD's band gap close to the CB edge, when calculated in a polar solvent like benzonitrile (Figure S1, right panel).

The key role of the isothiocyanate ligands on the destabilization of the dye's occupied orbitals is confirmed by the trend in mutual shifts of the QD- and dye-originated states in solvents of different polarities, as shown in Figure 4. For both **BD-c** and **1a** complexes adsorbed on the $Cd_{33}Se_{33}$, a polar solvent significantly shifts the dye-associated orbitals with respect to the QD's states. However, in the complex **1a** with bpy ligands, the polar solvent shifts the orbitals of the complex to higher energies, while orbitals of **BD-c** with SCN ligands are shifted toward lower energies. In fact, the occupied orbitals of **BD-c** are nearly at the midgap of the QD when the system is calculated in vacuum, while they move away from the gap, deeper into the VB with increasing solvent polarity (from chloroform to benzonitrile; Figure 4, left panel). Accordingly, the unoccupied states associated with tpy ligands are shifted in the CB toward its edge, when the QD/BD is calculated in benzonitrile. For complex **1a**, this trend is reversed. This reverse shift of the dye's orbitals for QD/Ru(II)bpy versus QD/BD originates from an opposite charge on the complexes: +1 for the complex **1a** and −2 for **BD-c**. In fact, similar to the QD/BD, the composites with **3a** and **4a** complexes having −1 and −2 charge due to additional deprotonated carboxylate groups demonstrate a slight shift of the dye's occupied orbitals further away from the edge of the VB with increases in the solvent polarity, while the dye's unoccupied orbitals move inside the QD's gap. This confirms that the sign of the total charge of the dye is the key factor governing the trend of stabilization or destabilization of the dye's orbitals in polar media.

The energy gap of the QD is also affected by solvent, increasing by about 0.3–0.5 eV with the solvent polarity, which

dx.doi.org/10.1021/jz502017u | J. Phys. Chem. Lett. 2014, 5, 3565–3576

agrees with previous computational reports.[26,28] A polar solvent stabilizes the surface states of the QD, while negligibly impacting the states localized at the inner (core) part of the QD. This increases the energy gap of the QD, since its HOMO and, especially, its lowest unoccupied molecular orbital (LUMO) have a lot of surface character, as seen in Figure 2. However, the complex's orbitals are much more strongly affected by solvent than the QD's states due to the larger electrostatic dipole moment of the complexes, compared to the QD. Therefore, a polar solvent has a stronger effect on the complex's states than the QD's states, resulting in either stronger destabilization of electronic levels of the Ru(II)bpy complexes with a positive charge or stronger stabilization of states associated with the black dye holding a negative charge. Thus, our calculations suggest that solvents with different polarities can be used to tune a mutual alignment of the dye's versus the QD's orbitals.

Despite the fact the negative charge on the dye helps to align the dye's orbitals closer to the band gap of the QD in nonpolar or weakly polar solvents, the Ru-associated orbitals in the **3a** and **4a** dyes are further away from the edge of the VB in the case of QDs functionalized by Ru(II)bpy than in QD/BD composites, when calculated in chloroform. In addition, complete deprotonation of carboxylic groups might not take place in experimental samples, if pH is not controlled. As such, the negatively charged peripheral groups do not destabilize the dye's occupied orbitals as efficiently as the isothiocyanates, which are directly coordinated with the Ru(II) ion. To elucidate the role of the negative charge on the ligands coordinating the Ru(II) ion, we have modeled two derivatives of the **BD** with isothiocyanate groups substituted by Cl^-, $[Ru(cpt)(Cl)_3]^{-1}$, and by CO, $[Ru(cpt)(CO)_3]^{+2}$, as depicted in Figure 5. The effect of the Cl^- ligands is very similar to the SCN^- groups: the occupied orbitals originating from these ligands are destabilized and shifted up to the edge of the QD's VB. The multiple bonds of the SCN^- ligands seem to play an insignificant role in the orbital destabilization: the complex with the Cl^- ligands, which do not have any triple or double bonds, results in a similar destabilization as the **BD** with SCN^- ligands. In contrast, neutral CO groups, with stronger electron withdrawing character than the Cl^- group, greatly stabilize the Ru-ion orbital and shift it even deeper into the VB of the QD, as compared to the QD functionalized by **1** or **2** complexes in chloroform. Consequently, it is the negative charge of the coordinating ligand that controls the destabilization of the dye's occupied orbitals in the QD/dye composites.

We note that calculations presented in Figure 5 and in Figure S1 in the Supporting Information are obtained by the B3LYP functional, while our other calculations utilize CAM-B3LYP functional. Comparison of data for the QD/BD in Figure 4 and Figure 5 together with data for QD/**1a** and QD/**2a** depicted in Figure 2 and Figure S1 demonstrate that both functionals provide similar shapes for the projected DOS and qualitatively identical behavior of the electronic structure of the composites. However, CAM-B3LYP strongly overestimates the energy gaps of both the dye and the QD, due to a larger portion of HF exchange in the functional.[44] In contrast, B3LYP provides more reasonable gap estimates of about 3 eV for the $Cd_{33}Se_{33}$ and 2.5 eV for Ru(II)bpy dyes, which are in better agreement with available experimental data.[42,28,31,46] As such, the overall trend in relative energy alignments of QD's and dye's states is consistent, independent of the functional, although the absolute values of energies are off. Therefore, we can conclude that the

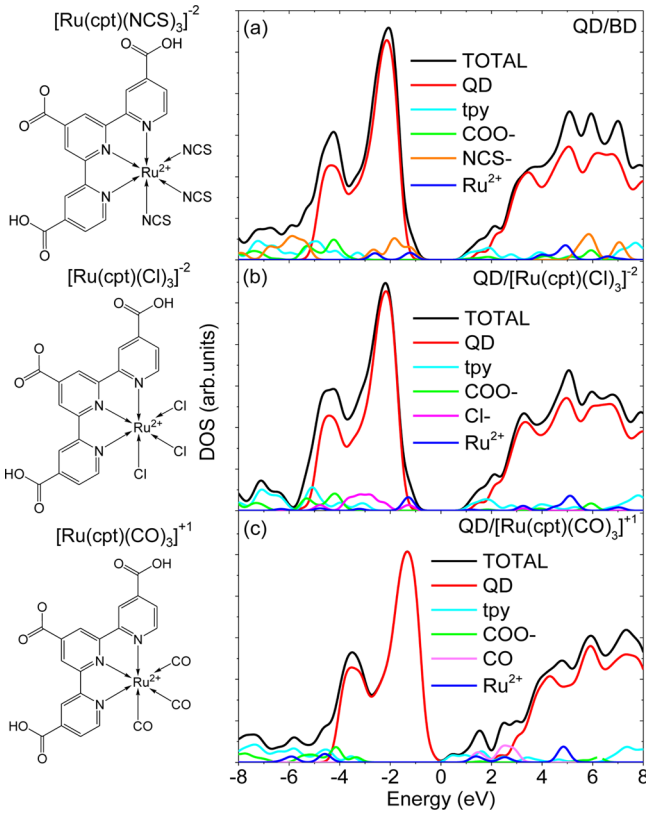

Figure 5. PDOS of $Cd_{33}Se_{33}$ functionalized by the **BD** (a) and its two derivatives where SCN^- are substituted by Cl^- (b) and CO (c) ligands. Left column depicts the schematic structures of complexes. PDOS is calculated by B3LYP functional in chloroform. B3LYP functional decreases the energy gaps, while the overall shape and structure of the PDOS stays the same as in CAM-B3LYP calculations. Neutral electron withdrawing CO groups strongly stabilize the dye's orbitals, while negatively charged Cl^- and SCN^- ligands destabilize the dye's orbitals shifting their occupied levels to the edge of the QD's valence band.

qualitative picture of the electronic structure of QD/dye composites is not changing with the functional. A similar conclusion for QDs was discussed in refs 26 and 44.

Confinement of charge carriers in the QD is expected to significantly affect the alignment of the dye's versus the QD's orbitals as well. To elucidate the effect of the QD's size, we compare the DOS of the large $Cd_{111}Se_{111}$ with the small $Cd_{33}Se_{33}$ clusters in vacuum and in the benzonitrile solvent, as depicted in Figure 6. As expected, an increase in the QD size from 1.5 to 2.2 nm leads to a smaller band gap. However, the confinement affects the CB more than the VB of the QDs. Thus, the VB edges have nearly equal energies in both small and large CdSe QDs, while the edge of the CB is red-shifted by about 2 eV in vacuum and 1.5 eV in solvent for the $Cd_{111}Se_{111}$. Such a difference in the VB and CB behavior originates from heavier holes, with the effective mass 4 times that of electrons in CdSe. Therefore, the VB edge is less sensitive to the confinement, compared to the edge of the CB. As such, it is reasonable to assume that, in the dye-functionalized QDs of a larger diameter, the occupied states associated with the dye are likely to stay at about the same position with respect to the VB as they are in smaller CdSe clusters. In contrast, the unoccupied orbitals of the dye likely occur deeper inside the CB of the QDs with diameters larger than 2 nm.

dx.doi.org/10.1021/jz502017u | J. Phys. Chem. Lett. 2014, 5, 3565−3576

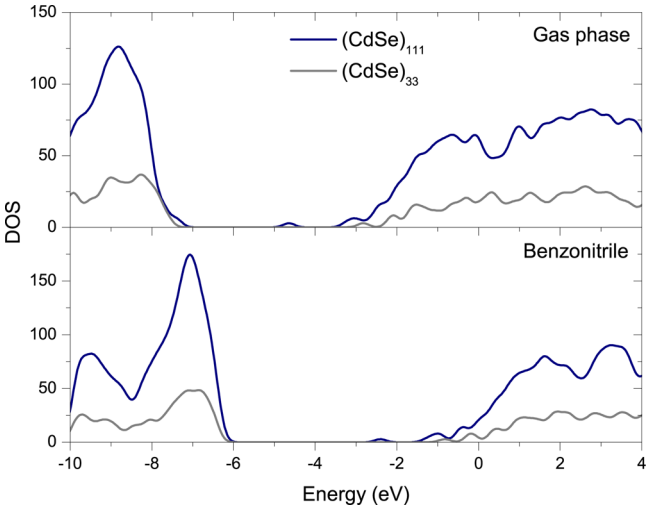

Figure 6. Comparison of the DOS for two sizes of bare QDs in vacuum (top) and benzonitrile solvent (bottom). Calculations are done by CAM-B3LYP functional. The DOS confirms what is expected from effective mass theory: As size increases, the band gap shrinks mainly through the conduction band of light electrons, moving closer in energy to the essentially static valence band formed by heavy holes.

Band Offsets: Role of QD−Dye Interactions. Experimentally it is challenging to directly determine the energy differences between HOMO of the dye and the QD in QD/dye composites. Therefore, these energy offsets are usually estimated from the electrochemical measurements of the isolated metal complexes and the QDs. The electrochemical measurements of $[Ru(II)(bpy)]^{+2}$ complex show an oxidation potential value of 1.26 V versus normal hydrogen electrode (NHE) in acetonitrile.[47] For many related complexes, the oxidation potential is estimated at the range of 0.69−1.77 V depending on the substituted ligands and experimental conditions.[48,49] The oxidation potentials for the CdSe QDs estimated from electrochemical and optical studies vary from 1.0 to 2.0 V vs NHE, depending on surface passivation, extent of traps, and even measurement conditions.[50] As such, by roughly judging from the measurements of the isolated components, the HOMO energy difference between the dye **1a** and the CdSe QD lays in the range from 1.2 to −0.2 eV, where the negative sign implies that the dye's HOMO is higher in energy than the HOMO of the QD.

Similarly, computational determination of the band offsets is a subject of many uncertainties, given the differences between the model used in the calculation and the actual experimental conditions. In the experiment, the QDs used are substantially larger than those used in the calculations. Additionally, the calculations are conducted at zero temperature and by approximating the solvent as a dielectric continuum, while the experiments have been performed under ambient conditions. However, since our calculations suggest that the VB edge of CdSe is not very sensitive to the size of the QD, the size difference in the QDs between calculations and experiments should not be of major consequence for determining the HOMO offsets. Thermal fluctuations could also affect the results; however, our calculations were performed at the equilibrium geometry, and most fluctuations should occur around this geometry leading to an averaging out of the fluctuation effects. Lack of explicit solvent molecules in the calculations could also affect the quality of our results. For the properties in which we are interested, however, the dominating contribution from the solvent should be from electrostatics rather than, for instance, hydrogen bonding. Since the absolute values of the electronic energies are not accurate reference values, we have chosen the lowest energy of a core 1s electron of the carbon from the methane group in the dye **1a** and in the phosphine oxide ligands passivating the $Cd_{33}Se_{33}$ surface as the reference point for both isolated systems. For the non-interacting dye and the QD, the calculated energy difference between their HOMOs varies from 0.03 to 0.5 eV depending on a solvent (see Table 1), which is in a reasonable agreement with the experimental values discusses above (ranging from −0.2 to 1.2 eV). This demonstrates an acceptable qualitative validity of used methodology despite all approximations. Compared to the $Cd_{33}Se_{33}$/**1a** case, calculations of the isolated black dye and the $Cd_{33}Se_{33}$ cluster show the offset occupied energies to be negative, i.e., the BD's HOMO is by ∼4.5 eV higher than the HOMO of the QD, which slightly increases for less polar solvents like chloroform, as shown in Table 1.

Having established the consistency between experimental and calculated values for band offsets for individual components, we further notice that the calculated difference between the HOMO associated with $Cd_{33}Se_{33}$ and **1a** (or **BD**) in the *interacting* QD/1a (or QD/BD) complex substantially changes when compared to *noninteracting* case as summarized in Table 1. Specifically, as shown in Figures 2, S1, and Table 1, the HOMO predominantly originating from the **1a** molecule is more negative by about 1.2 eV than the edge of the QD's VB, when calculated in chloroform and by 1.0 eV in benzonitrile. Similarly, interactions between the QD and the dye dramatically stabilize the dye's HOMO to about 0.2 eV below the QD's HOMO in QD/BD composites in polar solvents. Our observations suggest that electrostatic dipole−dipole coupling (more generally Coulombic interaction of

Table 1. Difference between Energies of the Highest Occupied Orbitals of the Dye and the QD (ΔE = $HOMO_{QD}$ − $HOMO_{dye}$) in eV and the Dipole Moments (μ) in Debye[a]

	QD-ligated/1a					QD/BD			
solvent	ΔE_{nonint}	ΔE_{int}	$\mu_{QD-nonint}$	$\mu_{dye-nonint}$	μ_{int}	ΔE_{nonint}	ΔE_{int}	$\mu_{dye-nonint}$	μ_{int}
chloroform	0.03	1.19	21.57	113.30	81.00	−4.55	−0.35	87.13	44.78
benzonitrile	0.46	1.01	22.53	114.98	82.03	−4.44	0.19	87.71	47.45
acetonitrile	0.47	1.00	22.61	115.10	82.09	−4.46	0.24	87.75	47.65

[a]Two cases are compared: the non-interacting (ΔE_{nonint}, $\mu_{QD-nonint}$, and $\mu_{dye-nonint}$) isolated and optimized complexes **1a**, **BD**, and the $Cd_{33}Se_{33}$ passivated by $OPMe_3$ ligands versus the interacting (ΔE_{int} and μ_{int}) QD/dye composites of the ligated $Cd_{33}Se_{33}$ functionalized by **1a** (QD-ligated/1a) and by BD (QD/BD) dyes. For the QD/BD composite, the QD is not ligated by $OPMe_3$. For each isolated systems, the energy of the HOMO is taken with respect to the energy of the core 1s electron of the carbon in a methane group. All calculations are performed with B3LYP functional and LANL2DZ(heavy atoms)/6-31G*(light atoms) basis set.

dx.doi.org/10.1021/jz502017u | J. Phys. Chem. Lett. 2014, 5, 3565−3576

Table 2. Difference between Energies of the Highest Occupied Orbitals of the Dye and the QD (ΔE = $HOMO_{QD}$−$HOMO_{dye}$) and the Dipole Moments (μ) of $Cd_{33}Se_{33}$/1a Composites in Different Solvents with the Complexes 1a Attached to Different Surfaces Labeled As A, B, and D[a]

	acetonitrile		benzonitrile		chloroform	
surface	ΔE (eV)	μ (Debye)	ΔE (eV)	μ (Debye)	ΔE (eV)	μ (Debye)
A	0.93	92.60	0.95	92.43	1.06	89.90
B	0.90	103.09	0.93	103.02	0.95	101.86
D	0.98	86.62	0.98	86.58	1.12	85.78

[a]All calculations are performed with B3LYP functional and LANL2DZ(heavy atoms)/6-31G*(light atoms) basis set.

inhomogeneous electronic densities) between the QD and the dye are responsible for these stabilization of the dye's orbitals with respect to the QD's VB edge. This effect is similar to the energy reorganization in polar solvent, when the electrostatic interactions between solvent molecules and a solute results may lead to a significant stabilization of electronic levels of a system.

In our case, both the dye and the QD have strong dipole moments, as recorded in Table 1. In fact, the calculated dipole moment of the CdSe QD is about 22−23 D, increasing with the solvent dielectric constant, which remarkably agrees with the experimental values of dipole moments of CdSe colloidal QDs measured as 25 and 47 D for 3 and 5 nm diameter nanocrystals.[51] The dipole moments of dyes is much higher. However, in the interacting system, the total dipole moment of the QD/dye composite becomes 1.5−2 times smaller than those of the isolated dye. This signifies a redistribution of the electronic density of the composite and results in stabilization of dye's orbitals. To decrease the dipole moment of the dye's part in the QD/dye composite, the electronic charge density should shift toward the Ru(II) center, rather than to the linking carboxylate group, leading to a more localized character of the dye and QD associated orbitals in composites, despite relatively strong dye-QD interactions. Overall, our results clearly demonstrate the dominating role of the QD-dye interactions on the mutual alignment of their electronic levels, resulting in stabilization of the dye orbitals with respect to the QD's VB edge. Subsequently, the energy offsets in the composites does not represent a simple difference of the isolated metal complexes and the QDs, which should be accounted for in experimental studies.

Indeed, the stabilization effect observed in our modeling is qualitative given a limited number of configurations considered. In the realistic systems these shifts are expected to depend on the detailed structure of the nanocrystal, attachment of the dyes with respect to the QD dipole moment direction, density of surface dye coverage, and ligand surface chemistry. While complex, this is expected to be an additional tunable parameter for arranging a favorable energetics in the future studies. Nonetheless, our calculations demonstrate that the attachment of the complex **1a** to different surfaces of the $Cd_{33}Se_{33}$ (A, B, and D surfaces illustrated in Figure S2 in Supporting Information) changes the HOMO offset energies by less than 0.1 eV, as depicted in Table 2. This small change in the energy alignments between the dye's and QD's HOMO is accompanied by a change in the total dipole moment by 5−15 D, depending on the interacting surface. Although the dependence of the dipole moment on the dye attachment is noticeable, it is much smaller than the change in the dipole moments associated with the QD−dye interactions (compare data in Tables 1 and 2), resulting in more significant changes in the energy offsets (0.6−1 eV) due to the QD−dye interactions than due to the adsorption of the dye to different QD's surfaces. The presence of the passivating ligands (Tables 1) also changes the offset energies by less than 0.1 eV, as compared to the case of the nonpassivated $Cd_{33}Se_{33}$ with the dye **1a** attached to the A surface shown in Tables 2. As such, the QD−dye interaction is the dominant factor in stabilization of the dye's levels with respect to the QD's states, while the surface chemistry of the QDs only slightly adjusts the energy offset values.

Thermodynamic Conditions for Charge Transfer. Overall, our calculations of the electronic structure of the dye functionalized $Cd_{33}Se_{33}$ suggest that the hole transfer from the photoexcited QD to Ru(II)bpy complexes with neutral ligands is thermodynamically unfavorable, since the QD associated states are higher in energy than the states associated with the Ru(II)bpy dye, as schematically illustrated in Figure 7, right

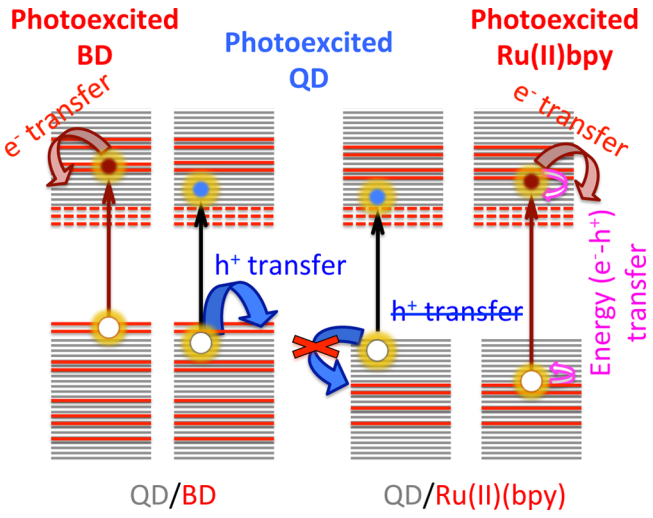

Figure 7. Schematic representation of the electronic structure of the QD/Ru(II)-dye composites illustrating the most probable charge transfer process. Left two panels describe processes in the CdSe QD functionalized by BD, when either the BD (first column) or the QD (second column) are excited. Right two panels describe processes in the CdSe QD functionalized by Ru(II)bpy, when either the QD (third column) or the Ru(II)bpy (fourth column) are excited. The states associated with the dye are red, and QD's states are gray. The lowest unoccupied states of the dyes are marked by dashed lines to depict their optically dark character originating from their metal-to-ligand charge transfer (MLCT) nature. The hole transfer from the QD to the dye is energetically favorable in QD/BD composites, while it is absolutely unfavorable in QD/Ru(II)bpy structures.

panel. In contrast, the occupied orbitals of the **BD** with the negatively charged ligands coordinated with the metal ion are comparable or slightly higher in energy than the QD's states at the edge of the VB. This energy alignment of the **BD's** orbitals provides favorable conditions for a photoexcited hole to transfer from the QD to the dye, as depicted in Figure 7, left panel.

Electron transfer from the photoexcited QD is also possible, since the dye's unoccupied orbitals are located below the QD's levels. Thus, both the electron and the hole transfer are thermodynamically favorable in QD/BD composites. In

dx.doi.org/10.1021/jz502017u | J. Phys. Chem. Lett. 2014, 5, 3565−3576

addition, the energy transfer process is also energetically possible in composites of small QDs. It was experimentally found that the energy transfer from the CdSe QD to the Ru(II)bpy dye dominates the charge transfer in QDs with diameters smaller than 4 nm.[10] In larger QDs, the energy of the CB edge decreases so that the unoccupied dye orbitals become higher in energy than the edge of the QD's CB, where the electron excitation occurs. Therefore, the electron transfer to the dye is less favorable in photoexcited QDs of diameter larger than 2 nm. When the dye is excited, the electron transfer from the dye to the QD is expected to dominate in QDs functionalized by the **BD** and its derivatives with negatively charged ligands. In composites of QDs functionalized by Ru(II)pby complexes with neutral ligands, however, the electron transfer has a higher chance to compete with the energy transfer, when both electron and hole are transferred from the complex to the QD, since the hole transfer is also energetically favorable in this case, as illustrated in Figure 7.

Similar scenarios for charge transfer have been experimentally detected in various functionalized QDs. For instance, experimental studies of CdSe QDs functionalized by rhodamine B (RhB) dyes have determined the predominant quenching pathway of exciton dissociation to be electron transfer from the RhB to the QD, while the energy transfer process from the complex to the QD accounted for 16%.[18] In CdSe QDs functionalized by Ru(II)bpy complexes, the hole transfer efficiency is still under debate, while the energy transfer from the complex to the QD has been clearly observed for QDs with diameter smaller than 4 nm.[10] An efficient hole transfer from the CdSe QD to the Ru(II) dye with the cyanide ligands (Ru505) has been detected by time-resolved PL spectroscopy and photocurrent measurements, independent of the presence of the TiO_2 substrate, while the energy transfer dominates in photoexcited QDs functionalized by the N3 dye with two thiocyanate ligands.[15,16] In CdS nanorods functionalized by $[Ru(II)bpy(tpy)Cl]^+$, the hole transfer from the photoexcited nanorods to the dye has been detected at the 0.1−1 ns time scale, while the electron transfer back to the CdS takes a much longer time (10−100 ns).[52]

If compared to the electron transfer from the anthocyanin-sensitized TiO_2 nanocrystalline films, where the electron injection from the dye to the semiconductor surface happens faster than 100 fs,[53] the observed times of the charge transfer in nonorode/dye composites[52] are much slower. Such relatively long times of charge transfer might be a signature of a weak Dexter type coupling between the donor and acceptor. As shown in Figure 3, our calculations demonstrate weak hybridization between the QD's and the dye's orbitals, despite a strong confinement of the QD, which is expected to force the QD's wave function to "leak" outside the QD surface. Due to the localized character of the dye and the QD orbitals, they do not strongly overlap, which should result in weak electronic couplings between subsystems leading to slower charge transfer. On the other hand, our simulations demonstrate the "leakage" of the QD's orbitals to small capping molecules, such as $OPMe_3$ or NH_2Me, resulting in a lot of QD−ligand hybridized states deep inside the VB and the CB of the QD.[29] As such, we conclude that it is the nature of the Ru(II) complexes that prevents strong hybridization with the QD states, despite significant QD−dye interactions and the QD confinement. Overall, our calculations point to the weak Dexter-coupling regime for QD/dye composites.

We would like to note, however, that our calculations only allow for estimations of thermodynamic conditions affecting the charge transfer, while kinetics and dynamics of charge transfer are left beyond our modeling. Indeed, many important characteristics, such as electronic donor−acceptor couplings, electron−phonon couplings, Auger couplings, and electron−hole couplings have to be directly calculated to provide a full description of the charge transfer in samples of QD/dye composites. To include these properties, nonadiabatic dynamics simulations[32,33] have to be performed to get all details on the charge and energy transfer, which is the scope of our future work. Nonetheless, the presented data on thermodynamic conditions allow us to roughly estimate the feasibility of charge transfer processes and their dependence on the type of the dye interacting with the QD surface. Thus, our calculations elucidate the effect of the dye structure on the minimal requirements to the Ru(II) complex molecules that either favor or disfavor the charge transfer in QD/dye composites.

Excited State Properties of QD/Dye Composites. The accuracy of charge/energy transfer measurements depends on the overlaps of optical transitions of each species in the hybrid QD/dye composites. The small overlap between optical transitions of the QD and the dye ensures better resolution and control in experiments. However, these overlaps are not only defined by the optical properties of individual molecules in the composite, but also by the QD−dye interactions. To explore the effect of the QD−dye interactions on the optical transitions of QD/dye composites, Figure 8 compares the absorption spectra of $Cd_{33}Se_{33}$ functionalized by the Ru(II)bpy complexes **1a** and the black dye **BD-t** and **BD-c** with the

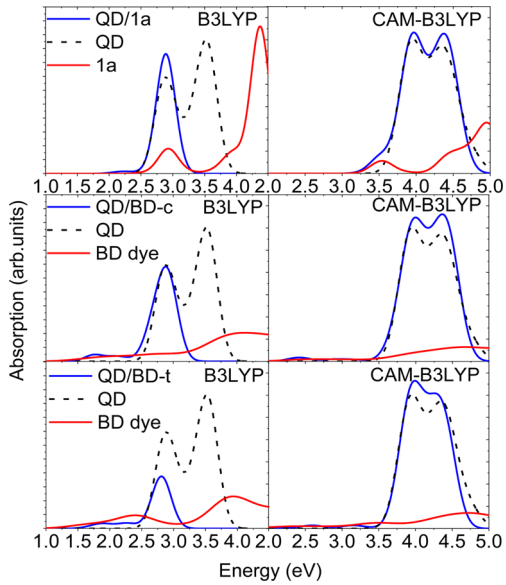

Figure 8. Calculated absorption spectra of the $Cd_{33}Se_{33}$ QD functionalized by Ru(II)−bipyridine complexes **1a** (top panels) and the black dye with different anchoring configurations (middle and bottom panels) in benzonitrile. For references, the absorption spectra of the bare $Cd_{33}Se_{33}$ QD (dashed black line) and the isolated Ru(II) complex (red line) are also plotted. Isolated systems are calculated with the preserved geometry they have in the hybrid QD/dye composite. Left and right panels compare the spectra calculated by hybrid B3LYP and by the long-range corrected CAM-B3LYP functionals. For all systems, the lowest-energy weakly intensive band are associated with the Ru(II) complex, which is very distinct from the next highly intensive band dominated by the QD transitions.

dx.doi.org/10.1021/jz502017u | J. Phys. Chem. Lett. 2014, 5, 3565−3576

respective spectra of the isolated pristine $Cd_{33}Se_{33}$ and dyes. This comparison clearly indicates the additive character of absorption spectra of composites: The main spectral features of the isolated systems coincide well with those of the functionalized QDs. The absolute values of the oscillator strengths of transitions contributing to each spectral peak for both isolated and interacting QD/1a systems are depicted in Figure S3 in the Supporting Information, directly evidencing the additive nature of the absorption spectra. Similar additive spectral character has been experimentally found in CdSe/Ru(II)bpy composites.[10] Such additive character is a signature of weak hybridization between the dye's and QD's orbitals contributing to optical transitions, explaining the weakly perturbed behavior of absorption spectra of QD/dye composites versus the isolated systems.

Figure 8 also compares the absorption spectra obtained by B3LYP and CAM-B3LYP functionals in order to check the effect of the used methodology on description of optical properties of the QD/dye composites. Overall, except the blue shift by about 1 eV in CAM-B3LYP calculations, both functionals provide qualitatively similar optical spectra of the systems, with a slightly blue-shifted dye component in QD/1a composite when calculated by B3LYP. In the considered QD/dye composites, the lowest-energy weak spectral peak belongs to the metal-to-ligand charge transfer (MLCT) transitions of the dye. Such low intensity, lower-energy states with MLCT character are typical for Ru(II) complexes.[42,43] In addition, there are a few low energy transitions in QD/dye composites that are optically dark, since they originate from the optically forbidden QD-to-complex transitions. The presence of these dark states in small CdSe QDs functionalized by dyes might significantly decrease the PL of composites.

The lowest energy dye-associated peaks are spectrally separated from the next highly intense band, mostly originating from optically active QD-to-QD transitions. This spectral separation should provide a good experimental resolution of the excitation of the Ru(II) complex. The **BD** has a smaller optical gap and wider absorption band compared to the Ru(II)bpy complexes.[54] All complexes demonstrate some overlaps between the higher energy dye and QD peaks in the absorption spectra of the QD/BD composites. Nonetheless, the second high-intensity band (at about 2.8 eV) in all composites we considered have predominantly QD character with just a small overlap with the dye's transitions. However, such overlaps between optical transitions originating from the dye and the QD are expected to increase in composites of larger size QDs, due to redshifts of the QD optical gaps.[26] Similar overlaps were experimentally found in QD/N3 composites,[15] which have a similar chemical structure to the BD. In this case, photoexcitation to the QD's absorption maxima cannot be uniquely assigned either to the QD or to the complex, and determination of the charge transfer process is very challenging in experimental probes.

To summarize, our DFT and TDDFT calculations demonstrate that variations in the solvent polarity and dye's ligands, specifically in their charge, can be tuned to adjust the electronic structure of QD/dye composites and, subsequently, to facilitate desirable conditions for charge transfer direction and efficiency. For instance, in considered molecular structures, functionalization of CdSe QDs by different Ru(II)bpy complexes with neutral ligands results in energetically unfavorable conditions for hole transfer from the photoexcited QD to the dye, since the occupied orbitals originating from the dye are located deeper inside the VB of the QD. In contrast, a substitution of bipyridines to thiocyanate ligands or Cl ions having negative charge, like in the black dye and its derivatives, destabilizes Ru(II)-associated orbitals, shifting them toward the very edge of the QD's VB. Such alignment of optically sensitive electronic levels allows for the energetically favorable conditions for the hole transfer from the QD to the black dye.

However, independent of the dye, its attachment, the QD size, and the presence of other small passivating ligands, the unoccupied orbitals of the dye appear close to the edge of the QD's conduction band. These states are linked to optically allowed MLCT transitions in the lowest energy absorption bands of the QD/dye composites, and provide pathways for electron transfer from the excited dye to the QD. In composites of CdSe QDs functionalized by Ru(II)bpy with neutral ligands coordinated to the metal ion, however, the electron transfer has a higher chance to compete with the energy transfer than in the QD/BD, since the hole transfer from the dye to the QD is also energetically favorable in this case. For larger QDs functionalized by Ru(II) complexes, our calculations predict the overlap between optically allowed dye-to-dye and QD-to-QD transitions in the absorption spectra of QD/BD composites, which make experimental control over the charge transfer direction very challenging. We also found that the mutual alignment of the dye's and the QD's orbitals is very sensitive to the solvent polarity. The dye's orbitals shift toward the lower energies with an increase of the solvent polarity in QDs functionalized by the dyes with negatively charged ligands, while the trends are reversed in composites of QDs functionalized by dyes with neutral ligands. These trends are attributed to the difference in the sign of the effective charge on the complex. As such, using less polar solvents for QD/BD composites is predicted to be more favorable for the energy level alignment to facilitate the hole transfer from the photoexcited QD to the black dye with negatively charged ligands. In contrast, more polar solvents are expected to provide more favorable conditions for the electron transfer from the photoexcited dye to the QD in composites of CdSe QDs functionalized by Ru(II)bpy dyes with neutral ligands. Finally, the QD-dye interactions are found to dominate in stabilization of the dye's orbitals with respect to the QD's VB edge, as compared to the QD's and dye's HOMO offsets in the isolated QDs and Ru(II) complexes. Our simulations pinpoint the origin of the effect only qualitatively given a limited number of considered structures. In fact, observed electronic level stabilization can be used in future studies to further tune the composite energetics by varying density of dye coverage, arranging preferential binding of dyes to specific QD crystal surfaces, modifying the electronegativity of surface ligands, etc. Overall, our calculations can be useful for guiding rational design of metal−organic dyes to achieve efficient directional charge transfer processes, important for photovoltaics and photocatalysis.

■ ASSOCIATED CONTENT

Supporting Information

Figure S1 represents schematic structure and PDOS of $Cd_{33}Se_{33}$ functionalized by various derivatives of Ru(II)bpy dyes bearing different charge depending on the number of attached deprotonated carboxylate groups on the bpy ligands. Figure S2 represents details on the attachments of different dyes to different surfaces of the $Cd_{33}Se_{33}$. Figure S3 shows details on the oscillator strength of optical transitions in

dx.doi.org/10.1021/jz502017u | J. Phys. Chem. Lett. 2014, 5, 3565−3576

$Cd_{33}Se_{33}$ /1a composites. This material is available free of charge via the Internet at http://pubs.acs.org

AUTHOR INFORMATION

Corresponding Author

*E-mail: svetlana.kilina@ndsu.edu.

Notes

The authors declare no competing financial interest.

ACKNOWLEDGMENTS

The authors thank Sergei Ivanov and Wenfang Sun for fruitful discussions and comments. SK acknowledges financial support of the US Department of Energy (DOE) Early Career Research grant DE-SC008446. S.T. acknowledge support from the Center for Advanced Solar Photophysics, an Energy Frontier Research Center funded by the U.S. Department of Energy (DOE), Office of Science, Office of Basic Energy Sciences (BES). The work has been conducted in part at the Center for Integrated Nanotechnologies (CINT) at Los Alamos National Laboratory (LANL). We also acknowledge the support provided by the Center for Nonlinear Studies (CNLS) operated by Los Alamos National Security, LLC, for the National Nuclear Security Administration of the U.S. DOE under contract DE-AC52-06NA25396. For computational resources and administrative support, we thank the Center for Computationally Assisted Science and Technology (CCAST) at North Dakota State University and the National Energy Research Scientific Computing Center (NERSC) allocation award 86678, supported by the Office of Science of the DOE under contract No. DE-AC02-05CH11231.

REFERENCES

(1) Mora-Sero, I.; Bisquert, J. Breakthroughs in the Development of Semiconductor-Sensitized Solar Cells. *J. Phys. Chem. Lett.* **2010**, *1*, 3046−3052.

(2) Peter, L. M. The Gratzel Cell: Where Next? *J. Phys. Chem. Lett.* **2011**, *2*, 1861−1867.

(3) Kuang, D.; Klein, C.; Zhang, Z.; Ito, S.; Moser, J. E.; Zakeeruddin, S. M.; Grätzel, M.; Stable. High-Efficiency Ionic-Liquid-Based Mesoscopic Dye-Sensitized Solar Cells. *Small* **2007**, *3*, 2094−2102.

(4) Wang, Q.; Zakeeruddin, S. M.; Nazeeruddin, M. K.; Humphry-Baker, R.; Grätzel, M. Molecular Wiring of Nanocrystals: NCS-Enhanced Cross-Surface Charge Transfer in Self-Assembled Ru-Complex Monolayer on Mesoscopic Oxide Films. *J. Am. Chem. Soc.* **2006**, *128*, 4446−4452.

(5) Nazeeruddin, M. K.; Liska, P.; Moser, J.; Vlachopoulos, N.; Grätzel, M. Conversion of Light into Electricity with Trinuclear Ruthenium Complexes Adsorbed on Textured TiO_2 Films. *Helv. Chim. Acta* **1990**, *73*, 1788−1803.

(6) Pang, A.; Chen, C.; Chen, L.; Liu, W.; Wei, M. Flexible Dye-Sensitized ZnO Quantum Dots Solar Cells. *RSC Adv.* **2012**, *2*, 9565−9570.

(7) Hodes, G. Comparison of Dye- and Semiconductor-Sensitized Porous Nanocrystalline Liquid Junction Solar Cells. *J. Phys. Chem. C* **2008**, *112*, 17778−17787.

(8) Balzani, V.; Bergaminia, G.; Marchionia, F.; Ceroni, P. Ru(II)−Bipyridine Complexes in Supramolecular Systems, Devices and Machines. *Coord. Chem. Rev.* **2006**, *250*, 1254−1266.

(9) Treadway, J. A.; Moss, J. A.; Meyer, T. J. Visible Region Photooxidation on TiO_2 with a Chromophore Catalyst Molecular Assembly. *Inorg. Chem.* **1999**, *38*, 4386−4387.

(10) Sykora, M.; Petruska, M. A.; Alstrum-Acevedo, J.; Bezel, I.; Meyer, T. J.; Klimov, V. I. Photoinduced Charge Transfer between CdSe Nanocrystal Quantum Dots and Ru−Polypyridine Complexes. *J. Am. Chem. Soc.* **2006**, *128*, 9984−9985.

(11) Klimov, V. I. Spectral and Dynamical Properties of Multiexcitons in Semiconductor Nanocrystals. *Annu. Rev. Phys. Chem.* **2007**, *58*, 635−673.

(12) Sambur, J. B.; Novet, T.; Parkinson, B. A. Multiple Exciton Collection in a Sensitized Photovoltaic System. *Science* **2010**, *330*, 63−66.

(13) Semonin, O. E.; Luther, J. M.; Choi, S.; Chen, H.-Y.; Gao, J.; Nozik, A. J.; Beard, M. C. Peak External Photocurrent Quantum Efficiency Exceeding 100% via MEG in a Quantum Dot Solar Cell. *Science* 201, *334*, 1530−1533.

(14) Lee, J.-W.; Son, D.-Y.; Ahn, T. K.; Shin, H.-W.; Kim, I. Y.; Hwang, S.-J.; Ko, M. J.; Sul, S.; Han, H.; Park, N.-G. Quantum-Dot-Sensitized Solar Cell with Unprecedentedly High Photocurrent. *Science Rep.* **2013**, *3*, 1050.

(15) Gimenez, S.; Rogach, A. L.; Lutich, A. A.; Gross, D.; Poeschl, A.; Susha, A. S.; Mora-Sero, I.; Lana-Villarreal, T.; Bisquert, J. Energy Transfer versus Charge Separation in Hybrid Systems of Semiconductor Quantum Dots and Ru-Dyes as Potential Co-sensitizers of TiO_2-Based Solar Cells. *J. Appl. Phys.* **2011**, *110*, 014314-1−7.

(16) Mora-Sero, I.; Likodimos, V.; Gimenez, S.; Martinez-Ferrero, E.; Albero, J.; Palomares, E.; Kontos, A. G.; Falaras, P.; Bisquert, J. Fast Regeneration of CdSe Quantum Dots by Ru Dye in Sensitized TiO_2 Electrodes. *J. Phys. Chem. C* **2010**, *114*, 6755−6761.

(17) Huang, J.; Stockwell, D.; Huang, Z.; Mohler, D. L.; Lian, T. Photoinduced Ultrafast Electron Transfer from CdSe Quantum Dots to Re−Bipyridyl Complexes. *J. Am. Chem. Soc.* **2008**, *130*, 5632−5633.

(18) Boulesbaa, A.; Huang, Z.; Wu, D.; Lian, T. Competition between Energy and Electron Transfer from CdSe QDs to Adsorbed Rhodamine B. *J. Phys. Chem. C* **2010**, *114*, 962−969.

(19) Morris-Cohen, A. J.; Aruda, K. O.; Rasmussen, A. M.; Canzi, G.; Seideman, T.; Kubiakb, C. P.; Weiss, E. A. Controlling the Rate of Electron Transfer between a Quantum Dot and a Tri-Ruthenium Molecular Cluster by Tuning the Chemistry of the Interface. *Phys. Chem. Chem. Phys.* **2012**, *14*, 13794−13801.

(20) Yang, Y.; Rodriguez-Cordoba, W.; Lian, T. Ultrafast Charge Separation and Recombination Dynamics in Lead Sulfide Quantum Dot−Methylene Blue Complexes Probed by Electron and Hole Intraband Transitions. *J. Am. Chem. Soc.* **2011**, *133*, 9246−9249.

(21) Knowles, K. E.; Malicki, M.; Parameswaran, R.; Cass, L. C.; Weiss, E. A. Spontaneous Multielectron Transfer from the Surfaces of PbS Quantum Dots to Tetracyanoquinodimethane. *J. Am. Chem. Soc.* **2013**, *135*, 7264−7271.

(22) McArthur, E. A.; Godbe, J. M.; Tice, D. B.; Weiss, E. A. A Study of the Binding of Cyanine Dyes to Colloidal Quantum Dots Using Spectral Signatures of Dye Aggregation. *J. Phys. Chem. C* **2012**, *116*, 6136−6142.

(23) Koposov, A. Y.; Szymanski, P.; Cardolaccia, T.; Meyer, T. J.; Klimov, V. I.; Sykora, M. Electronic Properties and Structure of Assemblies of CdSe Nanocrystal Quantum Dots and Ru−Polypyridine Complexes Probed by Steady State and Time-Resolved Photoluminescence. *Adv. Funct. Mater.* **2011**, *21*, 3159−3168.

(24) Inerbaev, T. M.; Masunov, A. E.; Khondaker, S. I.; Dobrinescu, A.; Plamad, A. V.; Kawazoe, Y. Quantum Chemistry of Quantum Dots: Effects of Ligands and Oxidation. *J. Chem. Phys.* **2009**, *131*, 044106−1−6.

(25) Bloom, B. P.; Zhao, L.-B; Wang, Y.; Waldeck, D. H. Ligand-Induced Changes in the Characteristic Size-Dependent Electronic Energies of CdSe Nanocrystals. *J. Phys. Chem. C* **2013**, *117*, 22401−22411.

(26) Hedrick, M.; Mayo, M. L.; Badaeva, E.; Kilina, S. First Principle Studies of the Ground and Excited State Properties of Quantum Dots Functionalized by Ru(II)−Polybipyridine. *J. Phys. Chem. C* **2013**, *117*, 18216−18224.

(27) Albert, V. V.; Ivanov, S. A.; Tretiak, S.; Kilina, S. V. Electronic Structure of Ligated CdSe Clusters: Dependence on DFT Methodology. *J. Phys. Chem. C* **2011**, *115*, 15793−15800.

(28) Fischer, S. A.; Crotty, A. M.; Kilina, S. V.; Ivanov, S. A.; Tretiak, S. Passivating Ligand and Solvent Contributions to the Electronic

Properties of Semiconductor Nanocrystals. *Nanoscale* **2012**, *4*, 904−914.
(29) Kilina, S.; Ivanov, S.; Tretiak, S. Effect of Surface Ligands on Optical and Electronic Spectra of Semiconductor Nanoclusters. *J. Am. Chem. Soc.* **2009**, *131*, 7717−7726.
(30) Abuelela, A. M.; Mohamed, T. A.; Prezhdo, O. V. DFT Simulation and Vibrational Analysis of the IR and Raman Spectra of a CdSe Quantum Dot Capped by Methylamine and Trimethylphosphine Oxide Ligands. *J. Phys. Chem. C* **2012**, *116*, 14674−14681.
(31) Ben, M. D.; Havenith, R. W. A.; Broer, R.; Stener, M. Density Functional Study on the Morphology and Photoabsorption of CdSe Nanoclusters. *J. Phys. Chem. C* **2011**, *115*, 16782−16796.
(32) Kilina, S.; Velizhanin, K.; Ivanov, S.; Prezhdo, O.; Tretiak, S. Surface Ligands Increase Photoexcitation Relaxation Rates in CdSe Quantum Dots. *ACS Nano* **2006**, *6*, 6515−6524.
(33) Kilina, S.; Neukirch, A.; Habenicht, B.; Kilin, D.; Prezhdo, O. Quantum Zeno Effect Rationalizes the Phonon Bottleneck in Semiconductor Quantum Dots. *Phys. Rev. Lett.* **2013**, *110*, 180404−1−4.
(34) Koposov, A.; Cardolaccia, T.; Albert, V.; Badaeva, E.; Kilina, S.; Meyer, T. Tretiak, S.; Sykora, M. Formation of Assemblies Comprising Ru(II)polypyridine Complexes and CdSe Nanocrystals Studied by ATR-FTIR Spectroscopy and DFT Modeling. *Langmuir* **201**, *27*, 8377−8383.
(35) Isborn, C. M.; Kilina, S. V.; Li, X.; Prezhdo, O. V. Generation of Multiple Excitons in PbSe and CdSe Quantum Dots by Direct Photoexcitation: First-Principles Calculations on Small PbSe and CdSe Clusters. *J. Phys. Chem. C* **2008**, *112*, 18291−18294.
(36) Kasuya, A.; Sivamohan, R.; Barnakov, Y. A.; Dmitruk, I. M.; Nirasawa, T.; Romanyuk, V. R.; Kumar, V.; Mamykin, S. V.; Tohji, K.; Jeyadevan, B.; Shinoda, K.; Kudo, T.; Terasaki, O.; Liu, Z.; Belosludov, R. V.; Sundararajan, V.; Kawazoe, Y. Ultra-Stable Nanoparticles of CdSe Revealed from Mass Spectrometry. *Nat. Mater.* **2004**, 3, 99−102.
(37) Puzder, A.; Williamson, A. J.; Gygi, F.; Galli, G. Self-healing of CdSe Nanoctystals: First-Principles Calculations. *Phys. Rev. Lett.* **2004**, *92*, 217401-1−4.
(38) Gao, B.; Shen, C.; Yuan, S.; Yang, Y.; Chen, G. Synthesis of Highly Emissive CdSe Quantum Dots by Aqueous Precipitation Method. *J. Nanomat.* **2013**, *2013*, 138526-1−7.
(39) Puzder, A.; Williamson, A.; Zaitseva, N.; Galli, G.; Manna, L.; Alivisatos, A. The Effect of Organic Ligand Binding on the Growth of CdSe Nanoparticles Probed by ab initio Calculations. *Nano Lett.* **2004**, *4*, 2361−2365.
(40) Frisch, M. J, et al. *Gaussian 09*, revision B.01; Gaussian, Inc.: Wallingford, CT, 2009.
(41) Yang, P.; Tretiak, S.; Masunov, A. E.; Ivanov, S. Quantum Chemistry of the Minimal CdSe Clusters. *J. Chem. Phys.* **2008**, *129*, 074709.
(42) Badaeva, E.; Albert, V. V.; Kilina, S.; Koposov, A.; Sykora, M.; Tretiak, S. Effect of Deprotonation on Absorption and Emission Spectra of Ru(II)−bpy Complexes Functionalized with Carboxyl Groups. *Phys. Chem. Chem. Phys.* **2010**, *12*, 8902−8913.
(43) Albert, V. V.; Badaeva, E.; Kilina, S.; Sykora, M.; Tretiak, S. The Frenkel Exciton Hamiltonian for Functionalized Ru(II)−bpy Complexes. *J. Lumin.* **2011**, *131*, 1739−1746.
(44) Azpiroz, J. M.; Ugalde, J. M.; Infante, I. Benchmark Assessment of Density Functional Methods on Group II−VI MX (M = Zn, Cd; X = S, Se, Te) Quantum Dots. *J. Chem. Theory Comput.* **2014**, *10*, 76−89.
(45) Cossi, M.; Rega, N.; Scalmani, G.; Barone, V. Energies, Structures, and Electronic Properties of Molecules in Solution with the CPCM Solvation Model. *J. Comput. Chem.* **2003**, *24*, 669−681.
(46) Nguyen, K. A.; Day, P. N.; Pachter, R. Understanding Structural and Optical Properties of Nanoscale CdSe Magic-Size Quantum Dots: Insight from Computational Prediction. *J. Phys. Chem. C* **2010**, *114*, 16197−16209.
(47) Kalyanasundaram, K. Photophysics, Photochemistry and Solar Energy Conversion with Tris(bipyridyl)ruthenium(II) and Its Analogues. *Coord. Chem. Rev.* **1982**, *46*, 159−244.
(48) Eskelinen, E.; Costa, P. D.; Haukka, M. The Synthesis and Electrochemical Behavior of Ruthenium(III) Bipyridine Complexes: $[Ru(dcbpy)Cl_4]$, (dcbpy = 4,4-dicarboxylic acid-2,2-bipyridine) and $[Ru(bpy)Cl_3l]$ (l = CH_3OH, PPH_3, 4,4-bpy, CH_3CN). *J. Electroanal. Chem.* **2005**, *579*, 257−265.
(49) Leigh, V.; Ghattas, W.; Lalrempuia, R.; Muller-Bunz, H.; Pryce, M. T.; Albrecht, M. Synthesis, Photo-, and Electrochemistry of Ruthenium Bis(bipyridine) Complexes Comprising a N-Heterocyclic Carbene Ligand. *Inorg. Chem.* **2013**, *52*, 5395−5402.
(50) Houtepen, A. J.; Vanmaekelbergh, D. Orbital Occupation in Electron-Charged CdSe Quantum-Dot Solids. *J. Phys. Chem. C* **2005**, *109*, 19634−19642.
(51) Blanton, S. A.; Leheny, R. L.; Hines, M. A.; Guyot-Sionnest, P. Dielectric Dispersion Measurements of CdSe Nanocrystal Colloids: Observation of a Permanent Dipole Moment. *Phys. Rev. Lett.* **1997**, *79*, 865−868.
(52) Tseng, H.-W.; Wilker, M. B.; Damrauer, N. H.; Dukovic, G. Charge Transfer Dynamics Between Photoexcited CdS Nanorods and Mononuclear Ru Water-Oxidation Catalysts. *J. Am. Chem. Soc.* **2013**, *135*, 3383−3386.
(53) Cherepy, N.; Smestad, G.; Gratzel, M.; Zhang, J. Ultrafast Electron Injection: Implications for a Photoelectrochemical Cell Utilizing an Anthocyanin Dye-Sensitized TiO_2 Nanocrystalline Electrode. *J. Phys. Chem. B* **1997**, *101*, 9342−9351.
(54) Hagfeldt, A.; Grätzel, M. Molecular Photovoltaics. *Acc. Chem. Res.* **2000**, *33*, 269−277.